An application of the dynamic deformation model to the tellurium isotopes

1987 J. Phys. G: Nucl. Phys. 13 161

(http://iopscience.iop.org/0305-4616/13/2/006)

J. Phys. G: Nucl. Phys. **13** (1987) 161–175. Printed in the UK

An application of the dynamic deformation model to the tellurium isotopes

A Subber†, W D Hamilton†, P Park†§ and K Kumar‡

† School of Mathematical and Physical Sciences, University of Sussex, Brighton BN1 9QH, East Sussex, UK

‡ Physics Department, Tennessee Technological University, Cookeville, TN 38505, USA

Received 14 April 1986

Abstract. The recent developments of the dynamic deformation model (DDM) make it readily applicable to a wide range of nuclei. We report a study of the even-mass tellurium isotopes from $N=68$ to the closed neutron shell at $N=82$. Within this region there is experimental evidence for nuclei with the characteristics of vibrational, rotational or γ-unstable level sequences. We show that the model is well able to account for these features as typified by level energies, electric quadrupole moments and γ-ray transition probabilities across this region when the only parameter which changes is the neutron number. For comparison the experimental data were also fitted to IBM-2 and the results from these fits are in general in good agreement with those from the DDM.

1. Introduction

The even-mass tellurium isotopes ($Z=52$) are part of an interesting region beyond the closed proton shell at $Z=50$ where the level structure has resisted detailed theoretical understanding. Although these nuclei were thought to be vibrational, the comparable strengths of the $2_2^+-2_1^+$ and the $2_2^+-0_1^+$ transitions in many isotopes and the systematic variation of the 0^+ level energy provides a clue suggesting that they might have a transitional character. Moreover, most of the measured quadrupole moments of the 2_1^+ states are non-zero and some are quite large [1, 2] with values that are comparable in magnitude with those of rotational nuclei. The early study of the collective potential-energy surface and nuclear structure of ^{124}Te, for example by Gneuss and Greiner [3], excluded a rotational behaviour since the level spectrum does not obey the $I(I+1)$ rule. A vibrational character was also excluded for this nucleus by the absence of a 0^+ level in the energy region of the two-phonon triplet. The γ independence of the potential-energy surface and level structure of some tellurium, xenon and barium isotopes were predicted at the same time by the Frankfurt group [4] and these features have been supported by several experimental and theoretical studies of ^{124}Te [5–7] and the recent identification of γ-unstable xenon isotopes [8]. The present investigation of the tellurium isotopes, $N=68-82$, mainly by the dynamic deformation model [9] is a part of a wider study which includes selenium, xenon and barium isotopes [10–12].

The dynamic deformation model has as its starting point the spherical shell model of Mayer and Jensen [13], in which the single-particle level energies are taken from the

§ Present address: Physics Department, University of Pittsburgh, Pittsburgh, PA, USA.

0305-4616/87/020161 + 15 $02.50

spectra of odd-A nuclei with one particle or hole outside a closed shell. These energies and the pairing strength are given a smooth dependence on N and Z so that there are no free parameters to be adjusted when the model is applied to any nucleus. Quadrupole deformations are introduced using the Rainwater [14] method. The potential energy of the deformation is obtained using the droplet model of Myers and Swiatecki [15] with a shell correction [16] and again there is only N, Z dependence. The nine collective variables (five quadrupole, neutron and proton energy gaps, and neutron and proton Fermi energies) are then treated by a time-dependent method introduced by Kumar [9]. The same Hamiltonian, operators and parameters are used for all even–even nuclei and the results for any particular nucleus are obtained specifying only N and Z.

The interacting proton–neutron boson model [17] IBM-2 was also applied to the same range of tellurium isotopes. We have used the same parameters as reference [18] to fit the energy while we estimated values for the effective charges e_ν and e_π in a way that will be discussed in § 2.4.

2. The dynamic deformation model

A full description of the DDM is given in reference [9] and references therein. Here we present only the results of our application of the new version [7] of the DDM to the tellurium isotopes.

Although the DDM has been applied to selected even–even nuclei ranging from light to heavy elements to study the gross feature of the collective spectra without any fitting parameters, more detailed systematic studies along a given chain of isotopes have not been carried out. Thus our analysis of tellurium isotopes represents a sensitive test of the DDM to discover if it contains the necessary mechanisms and has the sensitivity to describe in detail the changes in collective features of a wide range of isotopes.

2.1. The potential-energy surface

In figure 1 we define the limits of the geometrical picture of quadrupole oscillations in nuclei used in the DDM to describe the behaviour of the potential-energy surface [19]. They are also labelled with their corresponding IBM representations [20]. In addition a typical axial plot ($\gamma=0$ prolate and $\gamma=60°$, oblate) of the potential energy for each limit is also shown.

The potential-energy surfaces for the $N=70, 74, 82$ isotopes are given in figure 2 and the plots of the potential for $\gamma=0$, 30 and 60° against deformation β are given in figures 3 and 4. Both ^{122}Te and ^{124}Te have well defined minima at $\beta=0.2$ when $\gamma=0°$. However the form of the potential is quite different for these two nuclei as may be seen from figure 5, which shows a plot of the potential as a function of γ for constant β. The axial ($\gamma=0°$, or $\gamma=60°$) plots of the potential energy for $N=82$, 80, 78 76 and 72 isotopes which are used to construct the basic properties of the nuclear shape are shown in figure 6.

We shall begin our discussion with the $N=82$ nucleus and continue to the lighter isotopes. The potential-energy function $V(\beta, \gamma)$ gives circular contours, $V(\beta, \gamma) \sim \beta^2$, which are exactly what we expect from the model for a nucleus close to a doubly closed shell. The potential shape of this nucleus is that of a harmonic oscillator with a minimum in the potential at $\beta=0$. In the case of the $N=80$ isotope a shallow minimum of $V(\beta, \gamma)=0.35$ MeV appears at $\beta=0.05$ and $\gamma=0$, but unexpectedly a deep minimum of $V(\beta, \gamma)=7.9$ MeV occurs on the oblate axis at $\beta=0.09$. This deep minimum is surprising

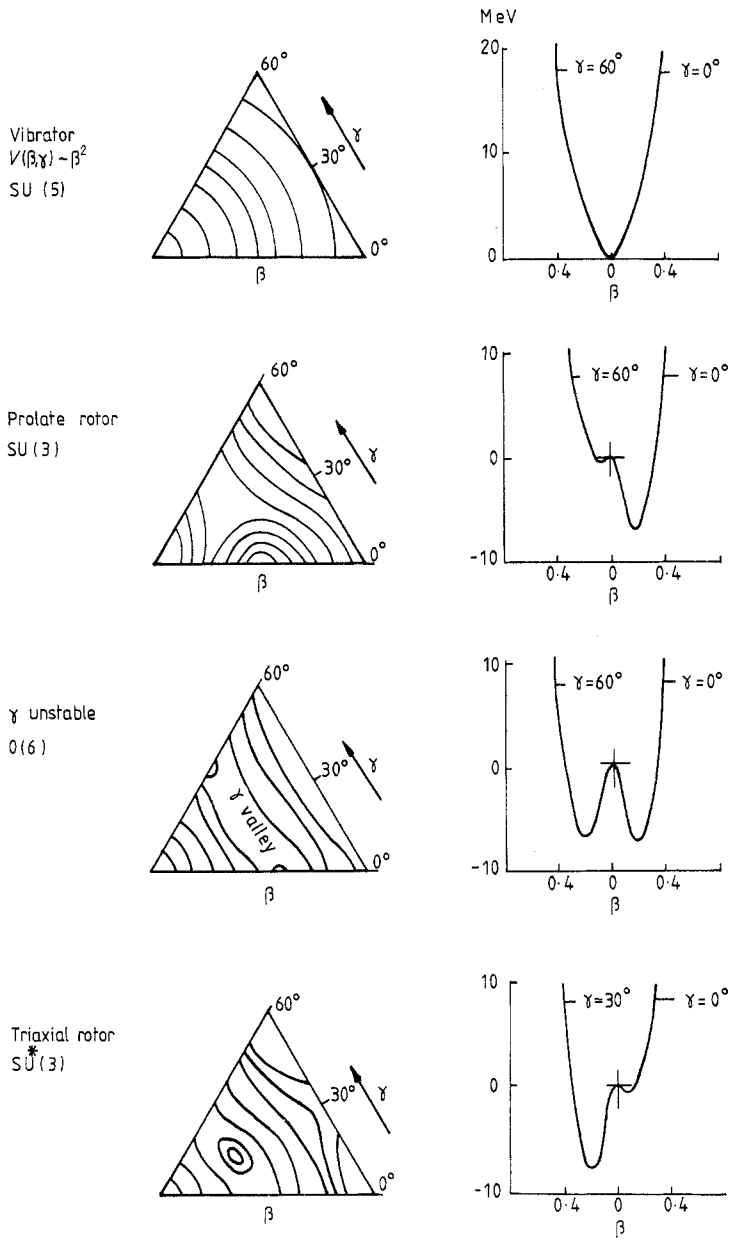

Figure 1. Four potentials used in the microscopic models are shown in a simplified form and their typical axial plots with limiting symmetries in the IBA model. The fifth type of the potential corresponds to an oblate rotor with the minimum at $\gamma \simeq 60°$. The value of the zero-point motion which determines the ground-state energy is omitted. In the case of a γ-unstable nucleus the ZPM energy will be greater than the energy difference between the two minima.

since only two neutrons have been removed and we might not expect such a dramatic change in the potential from that of the $N=82$ nucleus. However, we should note that this minimum is almost washed out by the 6.5 MeV energy of the zero-point motion. The potential well for $N=78$ shows stable minima for both oblate and prolate deformations.

It is soft against γ vibration but stiff against β vibration. Because of this the second excited 2^+ level will no longer belong to the band based on the first excited 0^+ band head but rather it will be the head of a γ-vibration band.

There is a little change in the general shape of the potential-energy function as we move to the $N=76$ isotope, but the nucleus does become increasingly γ soft as the minimum becomes increasingly deep. The same is true for the $N=74$ isotope. In the case of ^{124}Te ($N=72$) we have a typical example of the γ-unstable nucleus which may also be described by the O(6) limit in the IBM where the ground-state wavefunction is distributed over the whole range of γ values. Both the contour and the axial plots of the potential-energy surface of the $N=70$ isotope predict another good example of a γ-soft nucleus.

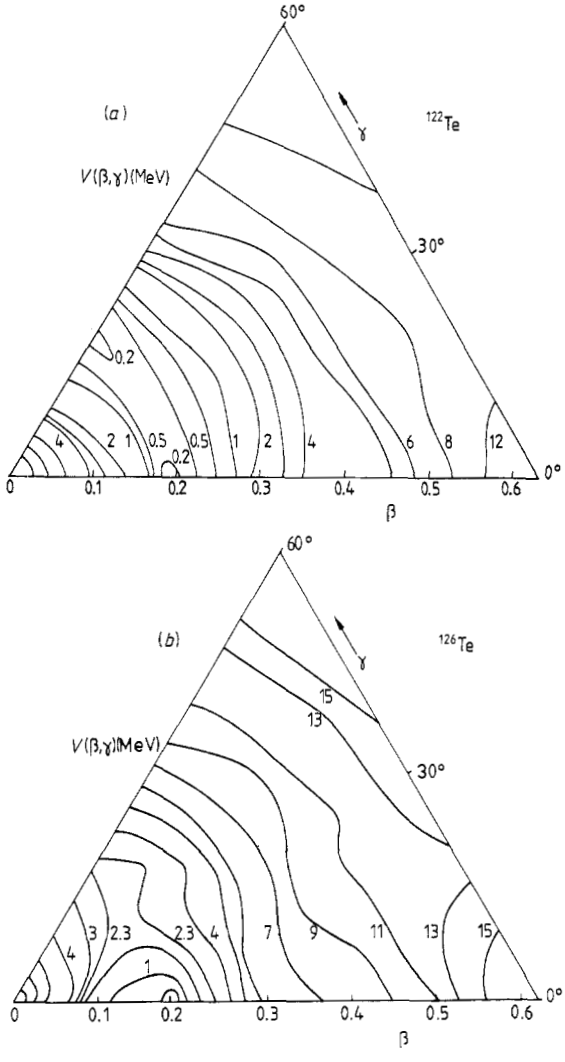

Figure 2. The contour plots show the theoretical potential-energy surface of $N=70$, 74 and 82 tellurium isotopes. The triangles are defined by the prolate edge which corresponds to $\beta_{min}=0$, $\beta_{max}=0.625$ and $\gamma=0°$ and the oblate edge which corresponds $\beta_{min}=0$, $\beta_{max}=0.625$ and $\gamma=60°$.

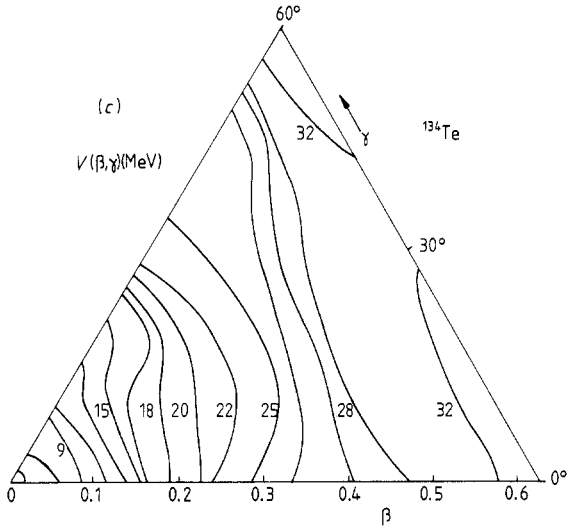

Figure 2. (*continued*)

An examination of the axial plots through the whole range of tellurium isotopes shows clearly that the $N=78$ and 76 isotopes are oblate. We also notice that with the decrease in neutron number the prolate minimum becomes deeper and moves to a larger β value. This

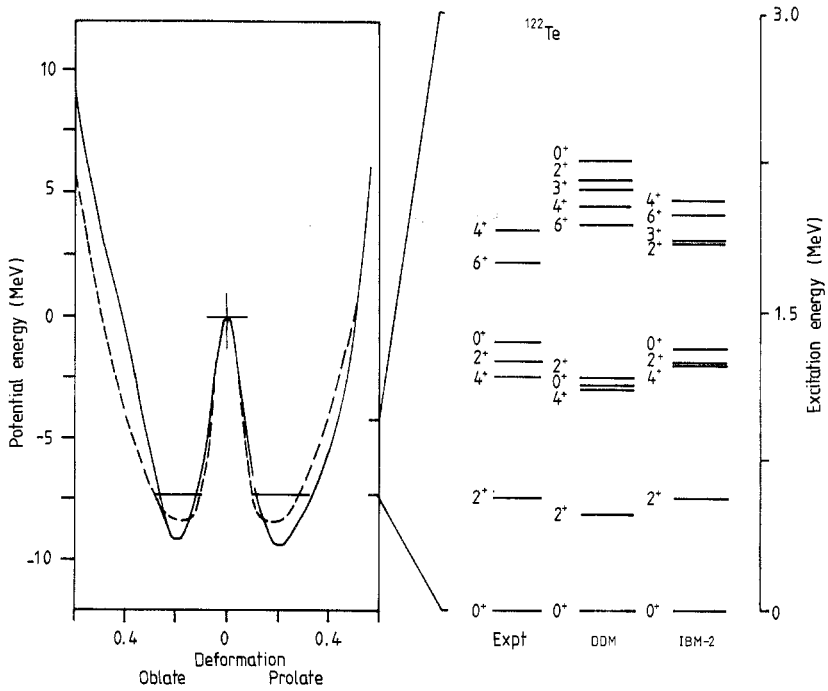

Figure 3. The plots show $E_{\text{def}}(\beta, \gamma=\text{fixed})$ against β for ^{122}Te and the experimental and theoretical DDM and IBM-2 energy levels. The horizontal lines represent the calculated ground-state energy which includes the energy of the zero-point motion. The broken curve corresponds to $\gamma=30°$.

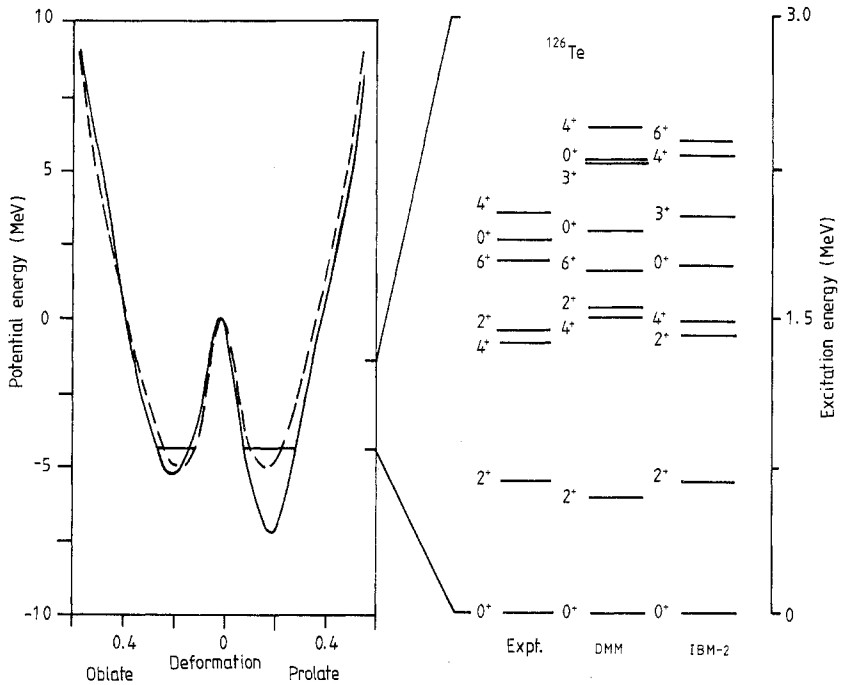

Figure 4. The plots show $E_{def}(\beta, \gamma = \text{fixed})$ against β for ^{126}Te and the experimental and theoretical DDM and IBM-2 energy levels. The horizontal lines represent the calculated ground-state energy which includes the energy of the zero-point motion. The broken curve corresponds to $\gamma = 30°$.

prolate shape is favoured for $N = 76$ while for $N = 72$ and 70 the two shapes are in equilibrium with comparable β and V_{min} values. We plot in figure 7 values of β corresponding to V_{min} as a function of neutron number as we proceed from the closed shell at $N = 82$. This illustrates the transition from a spherical nucleus ($N = 82$) through deformed γ-unstable nuclei ($N = 72, 70$) to the higher vibrational-like nuclei. We see a smooth increase in $\beta(V_{min})$ with decreasing neutron number for both prolate and oblate shapes. First the oblate shape dominates and beyond the γ-unstable region, where both shapes have the same deformation, the prolate shape is then the preferred one.

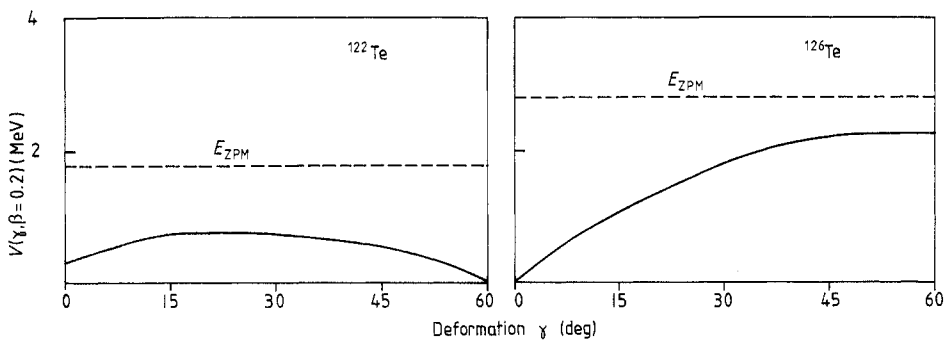

Figure 5. A cut in the potential-energy surface as a function of γ for constant $\beta = 0.2$ is shown for ^{122,124}Te. The potentials have been normalised to zero at their minima.

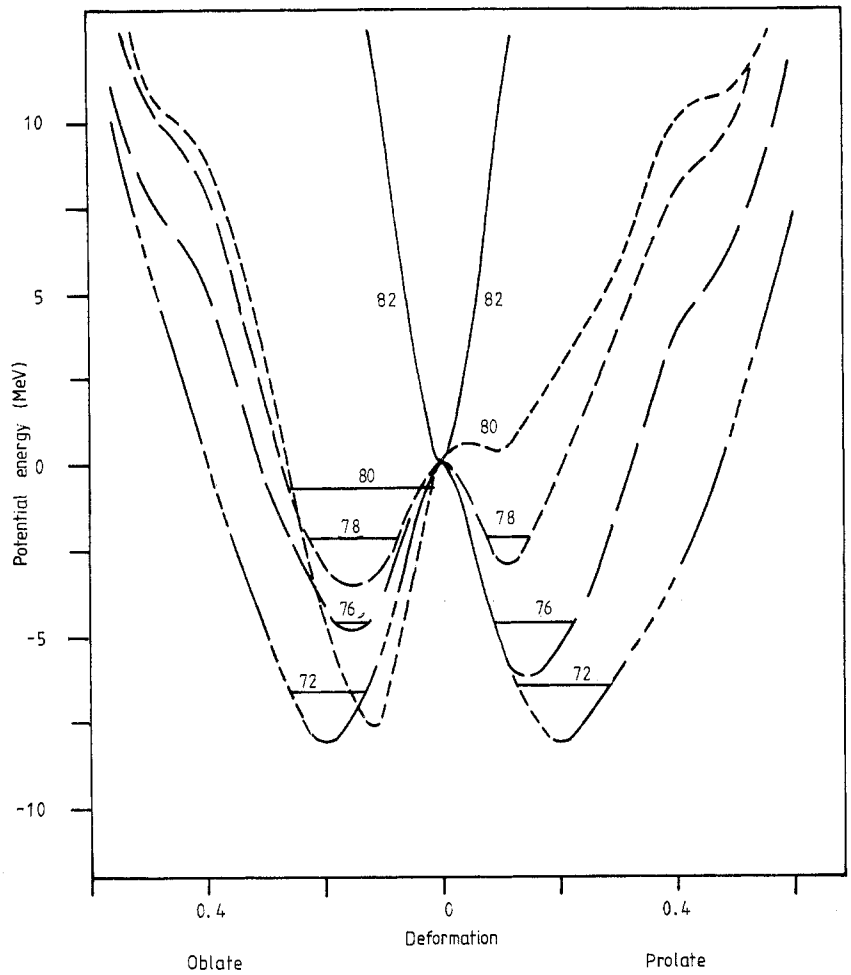

Figure 6. The deformation energies $E_{\text{def}}(\beta, \gamma = \text{fixed})$ for the tellurium isotopes $A =$ 124, 128, 130, 132, 134 are shown along the prolate and oblate axis. The energies are normalised to zero at $\beta = 0$ for all the isotopes. The horizontal lines represent the ground-state energies.

2.3. The level energies

The calculated collective energy levels of the tellurium isotopes were obtained by changing the value of N over the range $N = 68-82$ without adjusting any parameters in the model. In figures 3 and 4 we show the DDM experimental level energies for positive-parity states with $I \leqslant 6$ for the $N = 70$ and 74 isotopes. An IBM-2 fit is also presented in the same figure. DDM results are compared with the available experimental positive-parity states in figure 8 for the full range of isotopes. The behaviour of all of these states as a function of neutron number appears to be well reproduced by the DDM. However, the clear deviation of the 6^+ level from the typical behaviour of the collective energy spectrum as a function of neutron number could be related to a non-collective feature of this state especially near the closed shells at $Z = 52$ and $N = 82$. This may suggest the presence of some admixture in the wavefunction of this state from the two-quasiparticle configuration [21].

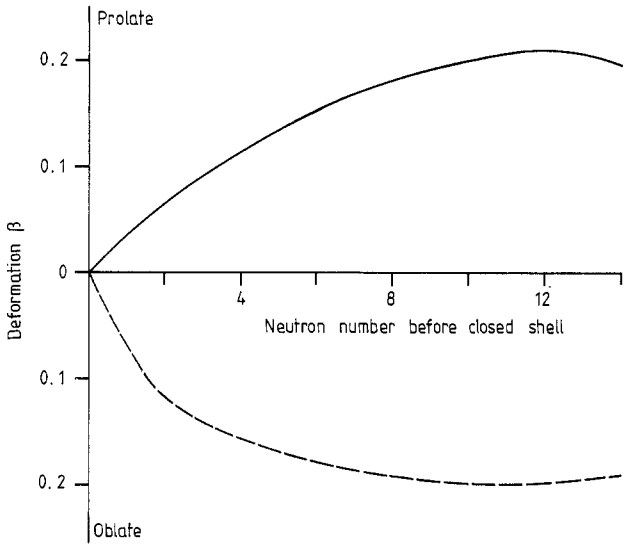

Figure 7. The plots show the deformation (β) at the potential minimum as a function of neutron number before the closed $N=82$ shell on both the prolate and oblate axis.

In the previous section we proposed that the potential-energy surfaces of ^{122}Te and ^{126}Te neighbours of the γ-unstable ^{124}Te nucleus also possess γ-unstable characters. As a consequence these nuclei will have degeneracies in levels with the same radial quantum number (n). Such degeneracies correspond to different representations, τ, of the O(5) symmetric group [6] with energy $E_{n\tau}$ and an approximate τ analysis of the DDM wavefunctions of 0^+ states have been made for these nuclei. We find that τ is an approximately good quantum number. For example in ^{122}Te the ground state is 96% ($\tau=0$), the first excited 0^+ state produced by the DDM at 1.14 MeV has 99% ($\tau=3$), while the second 0^+ excited state at 2.26 MeV has 92% ($\tau=0$). In the ^{126}Te nucleus the dominant components from the DDM are 94% ($\tau=0$) for the ground state, 84% ($\tau=3$) for the first excited 0^+ state at 1.91 MeV and 94% ($\tau=0$) for the second excited state at 2.26 MeV. If we take the experimental τ assignment to the 0^+ states to be $0_1^+(00)$, $0_2^+(10)$ and $0_3^+(03)$ then the DDM energy predictions for the two experimental 0_2^+ states in ^{122}Te and ^{126}Te at 1.36 and 1.87 MeV are too high by 0.9 and 0.4 MeV respectively, while the $\tau=3$ states are too low. However, if we assume the assignments to be like those of a typical spectrum of 0^+ states in the O(6) limit of the IBM [22, 23] then the DDM produces an impressive agreement with experiment without any parameter adjustment.

Figures 9–13 show the variation of some parameters of the tellurium isotopes from which we may draw the following conclusions.

(i) The microscopic quadrupole moment of the first excited state $Q(2_1^+)$ has a negative sign, figure 9, except for the two cases of $N=80$ and 82, where the sign changes to positive near the closed shell. Also the 2_2^+ state, which belongs to the first excited 0^+ band head, has a negative quadrupole moment in $N=68$, 80 and 82 (figure 10), which indicates that this 0_2^+ state is the head of a β-vibrational band. The quadrupole moment of this 2_2^+ state in the remaining isotopes has a positive sign and we thus conclude that the 2_2^+ in the $N=70$–78 range should belong to a different band or alternatively it may be the head of the γ-vibrational band. This feature is typical of the level structure of nuclei in the neighbourhood of γ-unstable nuclei.

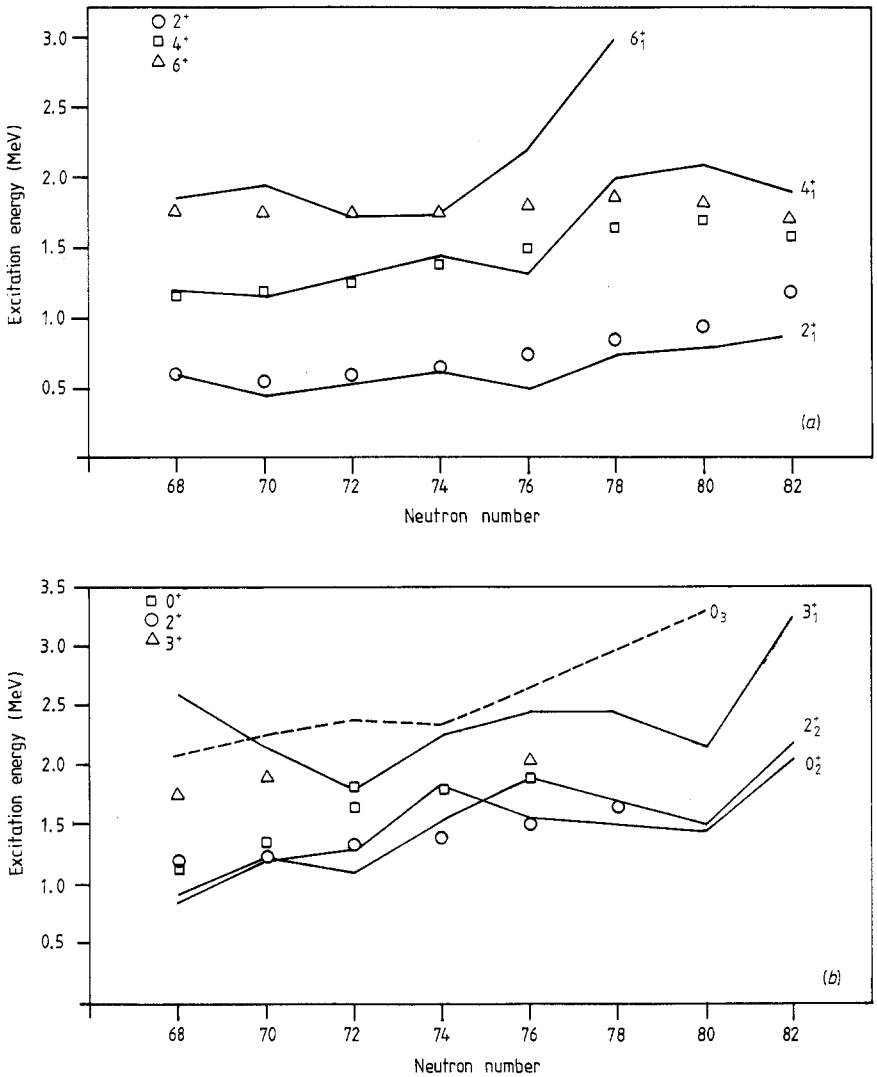

Figure 8. Experimental (points) and calculated energies for (*a*) the ground-state band and (*b*) some states of the quasibeta and quasigamma bands. The broken curve presents an alternative assignment for the systematic of the excited 0^+ state which has been made following the τ analysis of 0^+ states in these nuclei as explained in the text. The experimental points are from references [5, 24–28].

(ii) The $E(4_1):E(2_1)$ ratio (figure 11) of the level energies decrease from the maximum of 2.09 for $N=70$ to 1.23 for $N=82$. This indicates a non-collective quasiparticle excitation becoming increasingly important as the neutron number approaches $N=82$.

(iii) Both the experimental and calculated $E(4_1):E(2_2)$ ratios indicate that the 4_1^+ and 2_2^+ levels should occur close together throughout the range of isotopes from $N=68$–78.

(iv) The large values of the ratios $E(0_2):E(2_1)$ imply stiffness in the collective potential (figure 12) in the β degree of freedom which is consistent with the values in figure 13 for the deformation energy E_{def}.

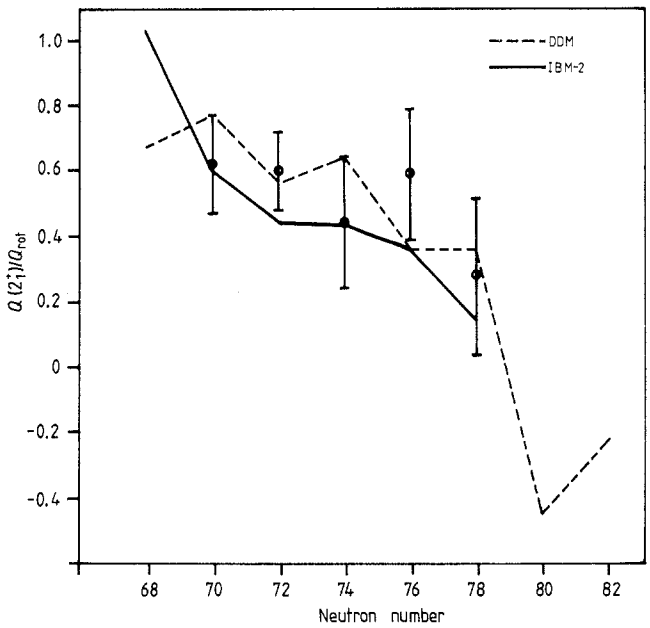

Figure 9. The quadrupole moments of the excited 2_1^+ state of tellurium isotopes relative to $Q_{rot} = \frac{2}{7}(16\pi B(E2; 2_1 - 0_1)^{1/2}$ are shown. The experimental data are taken from references [1, 2].

(v) The prolate–oblate energy difference E_{P-O} in figure 13 gives a measure of γ softness and the existence of a prolate or oblate shape for the ground state. Thus we see that the $N = 70$ and 72 isotopes are the most γ soft and that the prolate to oblate transition occurs between $N = 76$ and 78.

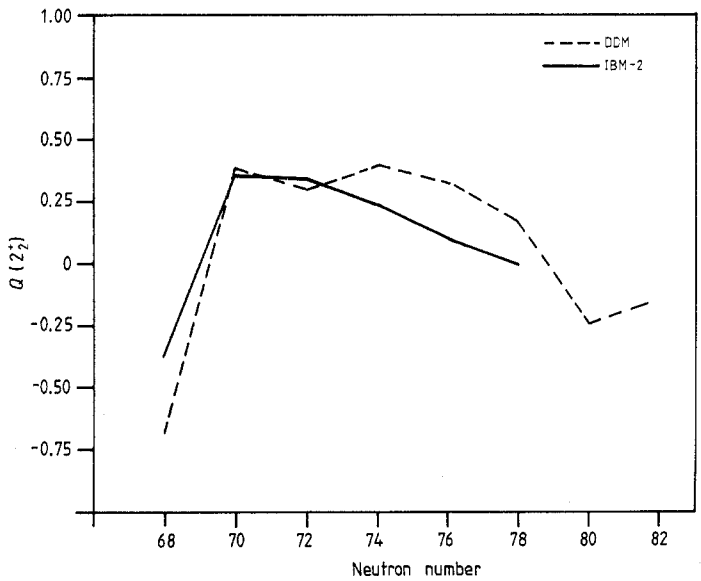

Figure 10. The behaviour of the quadrupole moment of the excited 2_2^+ in tellurium isotopes is shown as a function of neutron number N.

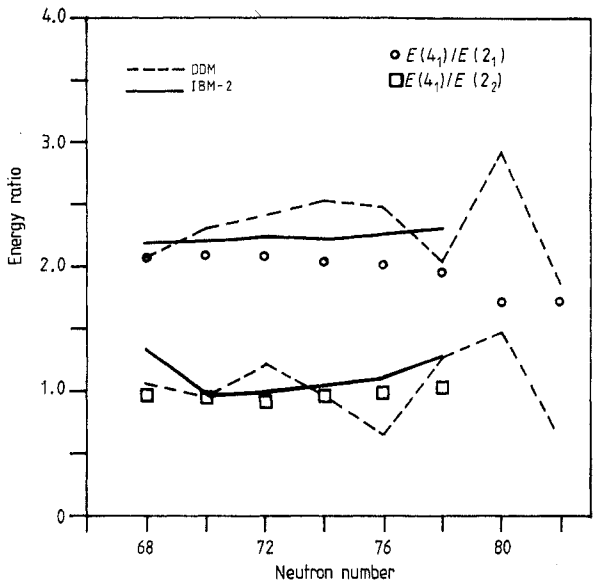

Figure 11. A comparison is made between calculated IBM-2, DDM and experimental $E(4_1):E(2_1)$ and $E(4_1):E(2_2)$ ratios for even-mass tellurium isotopes as a function of neutron number N.

(vi) The magnitude of the energy of zero-point motion changes from 1.8 MeV for $N=68$ to 16 MeV for $N=82$ as may be seen in figure 13. This gives an approximate measure of the overall stiffness of the collective potential-energy surface. For example for a spherical oscillator, the energy of the zero-point motion is given by $\frac{5}{2}h\omega$, where h is related to stiffness of the potential [9].

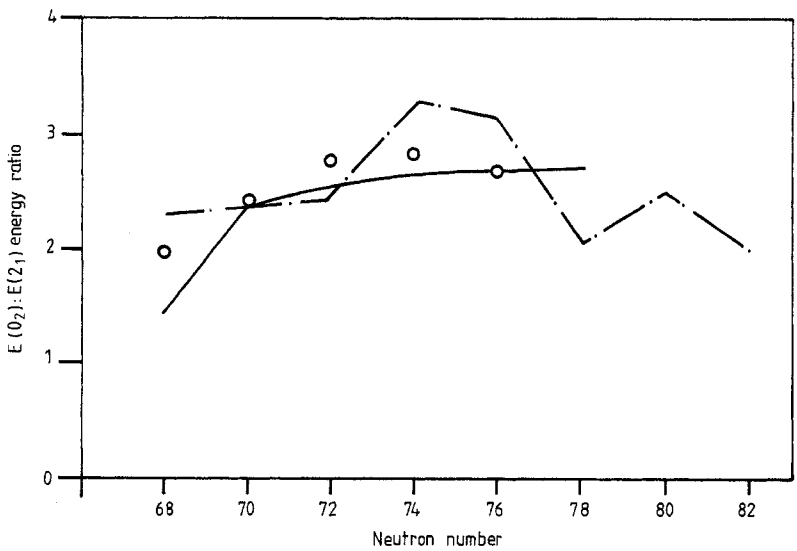

Figure 12. A comparison between calculated and experimental $E(0_2):E(2_1)$ ratio for even mass tellurium isotopes is shown as a function of neutron number N. The chain curve shows the DDM results and the full curve shows the IBM-2 results.

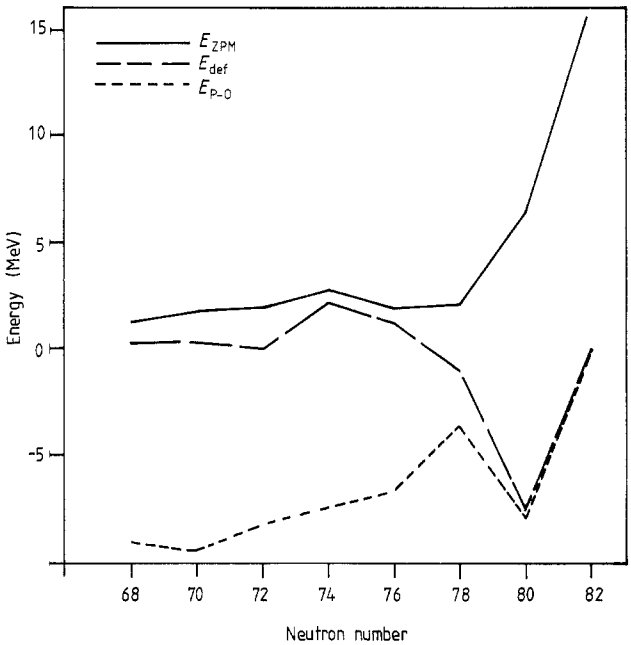

Figure 13. The DDM prediction for properties of the tellurium isotopes are plotted as a function of neutron number N. Energy of zero-point motion is denoted by E_{ZPM}, $E_{def}=E_{min}-E_{\beta=0}$ and E_{P-O} is the difference between the prolate and oblate minimum potential.

2.4. The absolute B(E2) values

The calculated $B(E2)$ values for transitions in the tellurium isotopes are presented in figure 14 together with the experimental values. Once more the agreement of DDM predictions with experimental values is good and it should be recalled that the DDM values are obtained without any fitting procedure or normalisation. The IBM-2 values were obtained by allowing the boson effective charges to vary with the neutron number (figure 15) within the area between two lines corresponding to the SU(5) and O(6) limits in IBM-1 (see figure 6 in reference [7]). Furthermore each calculated value was fitted to the corresponding measured $B(E2; 2_1^+-0_1^+)$ result for each of the isotopes. We see that these criteria provide $B(E2)$ values for other transitions which agree well with the DDM values and with experiments except for $2_2^+-0_1^+$ transitions in lower neutron number isotopes where the theoretical values in IBM-2 are about a factor of ten too small.

We note that since no parameter is adjusted in the DDM as we pass from one nuclear region to another as in most popular models, we cannot expect perfect agreement with the experimental data. Nevertheless, the potential-energy surface produced by the DDM is sensitive to the variation in neutron number through the chain of tellurium isotopes. The energies of experimental positive-parity states are well reproduced. Also $B(E2)$ transition probabilities and the collective quadrupole moments are generally in good agreement with the experimental data. The occurrence of the second 0^+ level occurs naturally in the DDM and higher 0^+ levels may be accounted for as collective levels without invoking the necessity of quasiparticle excitation. Altogether we believe that this study of the tellurium isotopes provides good evidence for the usefulness and quality of the DDM.

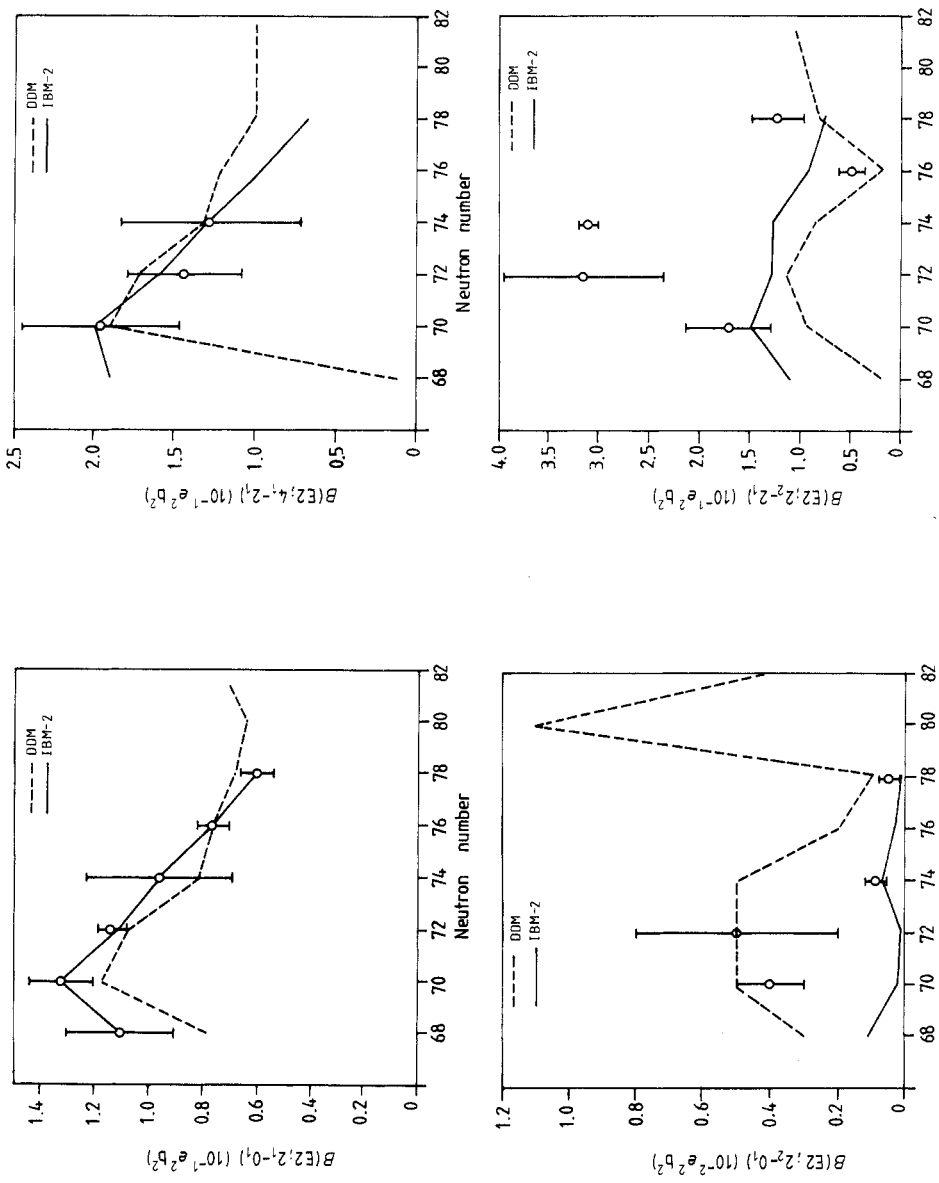

Figure 14. The calculated and experimental $B(\mathrm{E2}; I_i \to I_f)$ values are plotted, the experimental values are taken from references [2, 24].

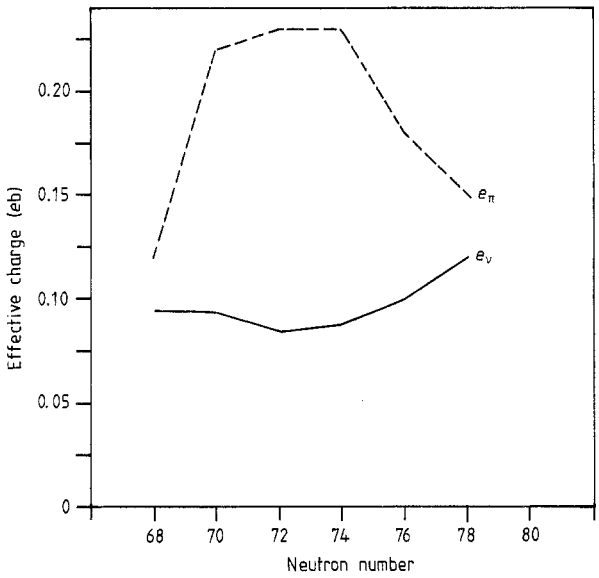

Figure 15. Neutron (e_ν) and proton (e_π) boson effective charges are plotted as a function of neutron number in tellurium isotopes. The two charges were chosen to fit $B(E2; 2_1 - 0_1)$ for each nucleus.

Acknowledgment

We are greatly indebted to Professor J P Elliott for many enlightening discussions.

References

[1] Larsen R D, Lutz W R, Ragland, T V and Scharenberg R P 1974 *Nucl. Phys.* A **221** 26
[2] Barrette J, Barrette M, Haroutunian R, Lamoureux G and Monaro S 1974 *Phys. Rev.* C **10** 1166
[3] Gneuss G and Greiner W 1971 *Nucl. Phys.* A **171** 449
[4] Arenhovel H, Gneuss G and Rezwani V 1971 *Phys. Lett.* **34B** 249
[5] Robinson S J, Hamilton W D and Snelling D M 1983 *J. Phys. G: Nucl. Phys.* **9** 961
[6] Park P, Subber A R H, Hamilton W D, Elliott J P and Kumar K 1985 *J. Phys. G: Nucl. Phys.* **11** L251
[7] Subber A R H, Park P, Hamilton W D, Kumar K, Schreckenback K and Colvin G 1986 *J. Phys. G: Nucl. Phys.* **12** 881
[8] Casten R F and Von Brentano P 1985 *Phys. Lett.* **152B** 22
[9] Kumar K 1984 *Nuclear Models and the Search for Unity in Nuclear Physics* (Bergen: University of Bergen Press)
[10] Subber A R H, Robinson S J, Hungerford P, Hamilton W D, Van Isacker P, Kumar K, Park P, Schreckenbach K and Colvin G G 1987 *J. Phys. G: Nucl. Phys.* to be published
[11] Hamada S A *et al* 1986 to be published
[12] Eid S A A *et al* 1986 to be published
[13] Mayer M G and Jensen J H D 1955 *Elementary Theory of Nuclear Shell Structure* (New York: Wiley)
[14] Rainwater J 1950 *Phys. Rev.* **79** 432
[15] Myers W D and Swiatecki W J 1974 *Ann. Phys., NY* **84** 186
[16] Stratinsky V M 1966 *Sov. J. Nucl. Phys.* **3** 449
[17] Otsuka T, Arima A and Iachello F 1978 *Nucl. Phys.* A **309** 1
[18] Sambataro M 1982 *Nucl. Phys.* A **380** 365
[19] Hess P O, Seiwert M, Maruhn J and Greiner W 1980 *Z. Phys.* A **296** 147

[20] Stephens F 1983 *Prog. Part. Nucl. Phys.* **9** 380
[21] Van Ruyven J J, Hesselink W H A, Akkermans J, Van Nes P and Herheul H 1982 *Nucl. Phys.* A **380** 125
[22] Arima A and Iachello F 1976 *Ann. Phys., NY* **99** 253; 1978 *Ann. Phys., NY* **111** 201
[23] Kane W R, Casten R F, Warner D D, Schreckenback K, Faust H R and Blakeway S 1982 *Phys. Lett.* **117B** 15
[24] Naqib I M, Christy A, Hall I, Nolan M F and Thomas D J 1977 *J. Phys. G: Nucl. Phys.* **3** 507
[25] Chowdhury P, Piel W F and Fossan D B 1982 *Phys. Rev.* C **25** 813
[26] Tamura T, Miyano K and Ohya S 1982 *Nucl. Data Sheets* **36** 227
[27] Kitao K, Kanbe M and Matumoto Z 1983 *Nucl. Data Sheets* **38** 191
[28] Lederer C M and Shirley V 1978 *Tables of Isotopes* (New York: Wiley)